Macromolecules

pubs.acs.org/Macromolecules Article

Impact of Polymer Rigidity on the Thermoresponsive Luminescence and Electron Spin Resonance of Polyester-Tethered Single Radicals

Liman Hou, Hongxue Xu, Xuanyu Zhang, Yipeng Zhang, Rui Chen, Zhaoyu Zhang, and Mingfeng Wang*

Cite This: *Macromolecules* 2022, 55, 8619−8628 Read Online

ACCESS | Metrics & More | Article Recommendations | Supporting Information

ABSTRACT: Stable organic radicals represent a unique type of functional materials for a broad scope of applications in optoelectronic and spintronic devices. A central challenge toward these applications is how to suppress the inter-radical aggregation that often causes aggregation-induced photoluminescence quenching and limits the correlation lifetime of the electron spins from the radicals. Here, we report an effective approach to fine-tuning luminescence and spin dynamics using a series of polyester-tethered single radicals, with a common core of carbazole-triphenylmethyl radical but different chains of polyesters with distinct glass transition temperature and rigidity. The rigidity of the polymeric matrices plays a critical role in tuning the luminescence and electron spin resonance of the radicals. The tunable properties of luminescence and electron spin dynamics as well as the robust photostability of such polymer-tethered single radicals represent important attributes for cutting-edge applications in optoelectronic devices and quantum information technologies.

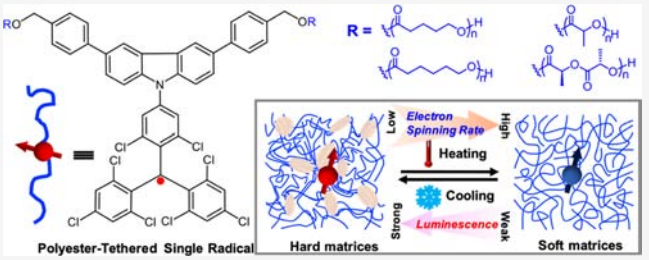

Organic radicals containing open-shell unpaired electrons have attracted tremendous attention due to their electronic and magnetic properties.[1−8] Recent developments have revealed unique emission characteristics of stable luminescent radicals based on their doublet states,[9−15] such as 100% (internal quantum efficiency in electroluminescent devices and the absence of the heavy metal effect.[11−15] They are also promising materials for spin-related information transmission, processing, and storage[16−18] due to their weak spin−orbit interaction and hyperfine interaction that results in long diffusion length of electron spins.

Control of intermolecular aggregation among organic radicals has been playing an important role in their physical properties in solid states. Existing systems to control intermolecular aggregation mainly rely on the dispersion of radicals in matrices of nonspin precursors. For example, to overcome the luminescence quenching caused by intermolecular aggregation in solid states of triaryl radicals, the radicals have to be diluted by physical dispersion in matrices of the nonspin radical precursors.[12,19] Similarly, the molecular packing in solid states shows a significant impact on the spin relaxation time of organic radicals, which is crucial to maintain spin polarization in quantum information processing. For example, to reduce the influence of intermolecular dipolar interactions on spin relaxation, Pei and co-workers[20] reported Rabi cycles with a remarkable coherence time beyond 1 μs under ambient conditions by dispersing triphenylmethyl radicals in a nonspin lattice of the radical precursors with a molar ratio of 1:1000. Overall, current methods of dispersing radicals in a nonspin lattice of the radical precursors, polymeric matrices, or molecular organic frameworks[21−23] still face challenges of tuning the inter-radical aggregation in a controllable and well-defined way.

Herein, we present an effective strategy for controlling inter-radical aggregation by covalently embedding single radicals into the middle of polymer chains. The intermolecular aggregation of the radical moieties in the polymeric matrices can be effectively suppressed once the polymer chains are long enough. This approach, with some resemblance to what is adopted by nature in fluorescent proteins, leads to bright photoluminescence (PL) with high quantum yields and robust photostability in rigid polymer matrices. Specifically, to study the impact of polymer rigidity on the physical properties of the tethered radicals, four types of representative polyesters, including poly(δ-valerolactone) (PVL), poly(ε-caprolactone) (PCL), poly(D,L-lactide) (PDLLA), and poly(L-lactide) (PLLA), were synthesized by controllable ring-opening polymerization (ROP) from a carbazole-substituted triphenylmethyl (CZ-TTM) radical as the initiator (Scheme 1). By changing the chemical structures of the polyesters, we found that the radicals tethered by polylactides with relatively high glass transition temperatures

Received: June 9, 2022
Revised: September 13, 2022
Published: September 30, 2022

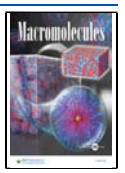

https://doi.org/10.1021/acs.macromol.2c01199
Macromolecules 2022, 55, 8619−8628

Scheme 1. Synthetic Routes to the Radical Initiator[a] (a) and Radical-Centered Polymers (b); (c) Schematic Presentation to Illustrate the Impact of Polymer Rigidity on the Luminescence and Electron Spin Dynamics of the Embedded Radicals

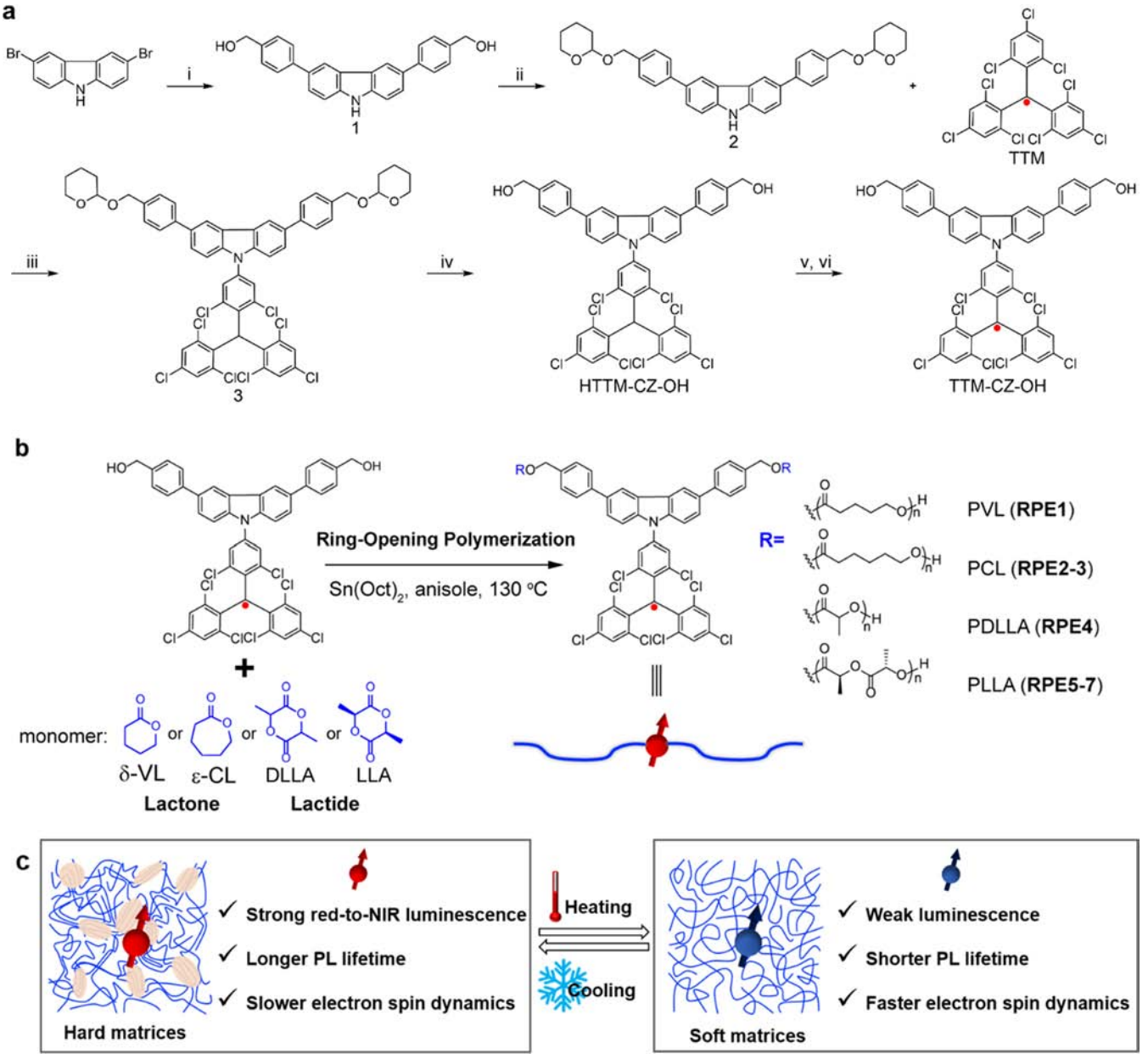

[a]Reagents and reaction conditions3 (i) (4-(hydroxymethyl)phenyl)boronic acid, K_2CO_3, $Pd(PPh_3)_4$, toluene, ethanol, H_2O, 1 °C; (ii) 3,4-dihydro-2H-pyran (DHP), *p*-toluenesulfonic acid monohydrate, tetrahydrofuran (THF), RT; (iii) Cs_2CO_3, dimethylformamide (DMF), 16 °C, N_2; (iv) HCl aq, THFFmethanol, 6 °C; (v) tetrabutylammonium hydroxide (TBAH) (2. M, methanol), THF, N_2, dark, RT; (vi) tetrachloro-*p*-benzoquinone, N_2, dark, RT.

(T_g) show strong red to near-infrared (NIR) PL in solid states under UV light (365 nm) at room temperature (RT), whereas the PL is turned of when the temperature is higher than T_g. The same radical centers tethered by polylactones, such as PVL or PCL exhibiting relatively low T_g are initially non-photo-luminescence at RT, but display strong PL after being cooled down by liquid nitrogen. Characterization by both optical spectroscopy and electron spin resonance (ESR) spectroscopy showed the absence of inter-radical aggregation of these polyester-tethered radicals in solid states. We further examined the impact of the rigidity of the polymer matrices on the PL of the tethered radicals by adding plasticizers that lower the T_g of the polymer matrices. Our results would of er a robust chemical tool for tuning the local environment of organic radical systems that determines their physical properties of PL and coherence of the spin relaxation for applications such as light-emitting devices and quantum information processing.

RESULTS AND DISCUSSION

Synthesis and Characterization. The synthetic route to the luminescent radical initiator TTM-CZ-OH is shown in Scheme 1a (see the Supporting Information for synthetic details). To introduce the hydroxyl group for polymerization, 3,6-dibromocarbazole was reacted with 4-benzyl alcohol boronic acid via a scheme of Suzuki cross-coupling to yield

https://doi.org/10.1021/acs.macromol.2c01199
Macromolecules 2022, 55, 8619−8628

the corresponding compound **1**. It is worth mentioning that in our initial attempt, the coupling of **1** to the tris(2,4,6-trichlorophenyl)methyl (TTM) radical using the classical method reported by Julia and co-workers[9] failed to produce the precursor of the radical initiator (i.e., HTTM-CZ-OH). In contrast, upon protection of the hydroxyl group with 3,4-dihydro-2H-pyran (DHP), compound **2** was reacted with TTM to yield compound (successfully, which was deprotected by hydrochloric acid to give HTTM-CZ-OH. Further reaction of HTTM-CZ-OH with tetrabutylammonium hydroxide (TBAH), followed by oxidation with 2,3,5,6-tetrachloro-*p*-benzoquinone gave the final radical initiator TTM-CZ-OH. The chemical structures of these intermediates were confirmed by proton nuclear magnetic resonance (^{1}H NMR) spectroscopy (Figures S1−S4). HTTM-CZ-OH and TTM-CZ-OH were further confirmed by electrospray ionization mass spectrometry (ESI-MS) (Figures S9 and S1).

The radical-centered polyester (RPE) polymers were prepared by ROP of δ-valerolactone (δ-VL) for RPE1, ε-caprolactone (ε-CL) for RPE2 and RPE3, D,L-lactide (DLLA) for RPE4, and L-lactide (LLA) for RPE5-7. Each of the polymerizations was initiated by a common radical initiator of TTM-CZ-OH using tin(II) ethylhexanoate ($Sn(Oct)_2$) as the catalyst. The chemical structures of the representative four kinds of polymers were confirmed by ^{1}H NMR (Figures S5−S8). The degrees of polymerization (DP) were determined by end-group analysis from the ^{1}H NMR spectra (Table 1), which match well with the number-average molecular weight (M_n) and polydispersity index (PDI) of the RPEs as characterized by gel-permeation chromatography (GPC) (Figure S11 and Table 1).

Figure S12 shows the differential scanning calorimetry (DSC) thermograms of the radical-centered polyesters. RPE1 shows a melting peak at 44 °C (Figure S12 and Table 1). RPE2 and RPE3 exhibit T_m values of 52 and 57 °C, respectively, corresponding to their molecular weight (MW) sequence. The T_g of RPE4 was found to be 28 °C. There is no melting peak for RPE4, indicating its amorphous nature in solid states. RPE5 shows a T_g at 23 °C, an exothermic peak at 86 °C (T_{cc}) attributed to cold crystallization, and three melting peaks at 123, 115, and 127 °C, respectively. The small melting peak before the melting peak of PLLA could be attributed to the melting of small and less perfect crystals. Both the T_m and T_g increase with the increase in molecular weights of RPE5, RPE6, and RPE7 (Figure S12 and Table 1).

The crystallinity of RPEs was measured by X-ray diffraction (XRD) (Figure S13). RPE1 exhibits characteristic diffraction peaks at 2θ values of 21.5 and 24.2°, corresponding to the crystallographic planes (11) and (20) of PVL,[24] respectively. RPE2 showed the characteristic crystallographic peaks at 21.3° (11) and 23.6° (20) of PCL.[25] The broad peak at 7−30° was attributed to the amorphous nature of PDLLA. RPE6 exhibits peaks at 2θ values of 14.7, 16.6, 18.9, and 22.3°, which are attributed to the PLLA crystalline phase.[26]

Optical Properties. We first characterized the optical properties of the representative radical-centered polyesters including RPE1, RPE2, RPE4, and RPE6 in solutions (toluene). All four RPEs exhibited the expected two characteristic absorption bands of the CZ-TTM unit (Figure 1a). The broad low-lying band with an absorption maximum at 620−630 nm is attributed to a charge transfer (CT) band from the electron-donating carbazole moiety to the electron-accepting trivalent carbon. A slight blue shift of the absorption band at 620−630 nm is observed in the polymer solutions, compared to that of TTM-

Table 1. Molecular Parameters and Thermal and Optical Properties of Radical-Centered Polyesters

						in toluene			thin films			
sample	composition[a]	$M_{n,NMR}$[a] (kg/mol)	$M_{n,GPC}$[b] (kg/mol)	PDI[b]	T_g (°C)	T_m (°C)	$\lambda_{max,abs}$ (nm)	$\lambda_{max,em}$ (nm)	Stokes shift (nm)	$\lambda_{max,abs}$ (nm)	$\lambda_{max,em}$ (nm)	Stokes shift (nm)	τ_{ave}[e]	Φ (%)
RPE1	PVL_{58}-TTM-CZ-PVL_{58}	18.9	9.7	1.18		44	629	712	83	626	721[c]/749[d]	95[c]/123[d]	2.4[c]/17.2[d]	2.2
RPE2	PCL_{48}-TTM-CZ-PCL_{48}	18.1	18.5	1.21		52	627	708	81	627	712[c]/739[d]	85[c]/112[d]	2.1[c]/14.7[d]	1.9
RPE3	PCL_{84}-TTM-CZ-PCL_{84}	28.8	36.2	1.36		57	627	707	80	625	705[c]/769[d]	75[c]/144[d]	2.4[c]/24.3[d]	2.4
RPE4	$PDLLA_{25}$-TTM-CZ-$PDLLA_{25}$	8.1	8.6	1.15	28		627	693	66	624	712[c]/758[d]	88[c]/84[d]	16.1[c]/16.4[d]	18.9
RPE5	$PLLA_{16}$-TTM-CZ-$PLLA_{16}$	5.6	5.2	1.28	23	103/115/127	624	703	79	621	705[c]/712[d]	84[c]/91[d]	14.5[c]/21.8[d]	15.5
RPE6	$PLLA_{25}$-TTM-CZ-$PLLA_{25}$	8.1	9.0	1.29	32	116/138	624	703	79	619	707[c]/750[d]	88[c]/90[d]	17.0[c]/22.8[d]	15.9
RPE7	$PLLA_{58}$-TTM-CZ-$PLLA_{58}$	15.3	11.6	1.24	41	142/150	626	703	77	625	697[c]/693[d]	92[c]/88[d]	18.4[c]/24.1[d]	16.0

[a]Subscripts denote the number-average degree of polymerization (DP), which was calculated from ^{1}H NMR. [b]M_n and polydispersity index (PDI) were determined by GPC. [c]At 78 K. [d]At RT. [e]Average photoluminescence lifetime.

https://doi.org/10.1021/acs.macromol.2c01199
Macromolecules 2022, 55, 8619−8628

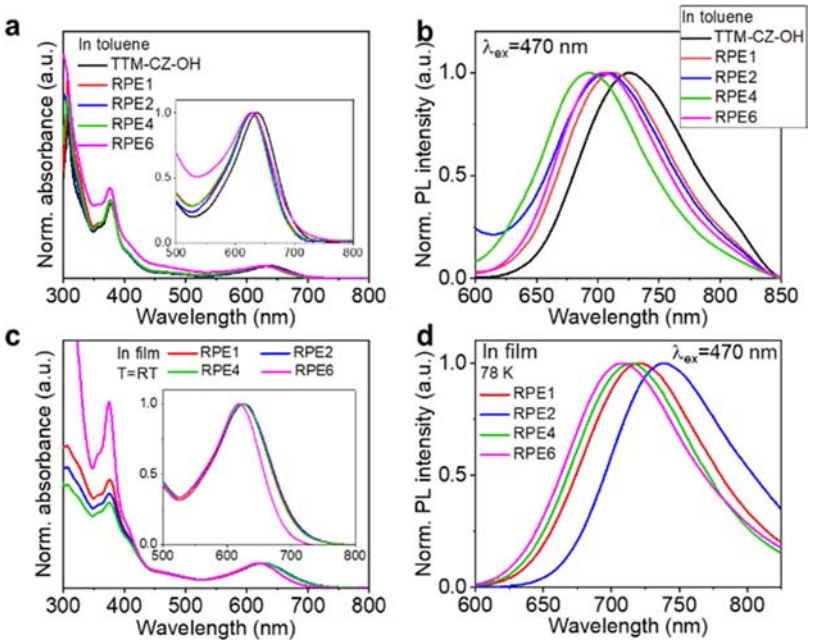

Figure 1. Normalized (abbreviated as Norm.) absorption (a, c) and steady-state PL spectra (b, d) of TTM-CZ-OH and four RPEs in toluene (1 mgF mL) (a, b) and as thin films spin-cast on quartz slides (c, d). The inset graphics magnify the absorption band centered around 62 nm.

CZ-OH in the same solvent (i.e., toluene). These results suggest that the attached polyester chains have some impact on the conformation and suppress 1exibility of the radical unit in toluene and that there is no obvious π−π aggregation between CZ-TTM units in a dilute solution of toluene. The digital photographs (Figure S14) show obvious red PL of the four RPEs in toluene under UV (365 nm) light irradiation.

The steady-state PL emission spectra (Figure 1b and Table 1) of RPE1, RPE2, RPE4, and RPE6 all show a broad peak with maximal emission ($\lambda_{max,em}$) in the range of 693−712 nm. The Stokes shifts (gap between the maximal absorption and emission wavelengths) follow the order of RPE4 J RPE6 J RPE2 ≈ RPE1 in toluene. Such a dif erence in the Stokes shift among the four RPEs could be attributed to the balance of multiple factors such as polarity[27] and rigidity (which re1ects the local free volume) of the polymers in solution.[28−3]

Next, we studied the optical properties of RPE1−RPE7 in f lms and bulk solid states. Figure S15 shows the digital photographs of TTM-CZ-OH and RPE1-RPE7 in bulk solid states (i.e., powders) under room light and UV (365 nm) light, respectively. It is clear that RPE4-RPE7 has bright deep-red emission in these solid states, whereas RPE1−RPE3 show dim red PL, and TTM-CZ-OH is non-photoluminescent at all. Figure 2a shows digital photographs of representative RPE1, RPE2, RPE4, and RPE6 in f lms. Red PL is only observed at a low temperature (e.g., cooled by liquid nitrogen) for RPE1−RPE3 (Figures 2a and S16). Such dif erent optical properties can be seen more quantitatively in the UVFvis absorption and steady-state PL emission spectra. RPE1 and RPE2 f lms showed similar UVFvis absorption to those of RPE4 and RPE6 (Figure 1c). The Stokes shifts follow the order of RPE4 J RPE6 J RPE1 J RPE2 at RT and RPE4 KRPE6 J RPE1 J RPE2 at 78 K (Table 1). The smaller Stokes shift in higher rigid polymer matrices could be attributed to the suppression of the intramolecular vibrationFrelaxation of the radicals.

Temperature-dependent steady-state PL emission spectra of representative RPEs are shown in Figures 2b and S18. When the temperature was decreased from 3 to 8 K in situ, the PL emission intensities of RPE1 and RPE2 increased gradually (Figures 2c and S18). A remarkable blue shift of the maximal emission wavelength can be observed for RPE1 (Figure S18) and RPE2 (Figure S17) upon decreasing the temperature. Compared to RPE1−2, the changes of both the PL intensities and the maximal emission wavelengths of RPE4 and RPE6 upon the change of temperature from 78 to 298 K were much less obvious (Figure S18c−f).

The results of the absolute photoluminescence quantum yields (denoted as PLL Y or Φ) for RPE1−RPE7 f lms are summarized in Table 1. The PLL Y for RPE1−3 was in the range of 1.9−2.4(at RT. A signif cant enhancement of Φ was observed for RPE4 (Φ K 1.9( ) and RPE5−7 (Φ K 15.5−16.( ). These results, consistent with the temperature dependence of the PL lifetimes, as discussed below, indicate that radicals dispersed in the soft polymeric matrices (RPE1−3) are more sensitive to temperature change than those in the rigid ones (RPE4−7).

We measured the PL lifetimes (τ) from the PL decay prof les of various RPEs at both RT and 78 K. The decays were f tted with the triple-exponential function at RT (Figures 2d−f and S19) and the monoexponential function at 78 K (Figure S2). The quality of the f tting was evaluated from weighted residuals below the PL decay prof les. The f tting results are presented in Table S1. The χ^2 were all below 1.3, which indicates the good quality of the f tting. The average lifetimes (τ_{ave}) for RPE1, RPE2, and RPE3 at RT were in the range of 2.1−2.4 ns (Figure 2d−f and Tables 1 and S1). While for RPE4−7 at RT, the τ_{ave} was increased from 14.5 to 18.4 ns. When the temperature was decreased to 78 K, the τ_{ave} for all RPEs increased to the range from 14.7 to 24.3 ns (Figure S2 and Tables 1 and S1). Such an increase in the PL lifetime is consistent with the increase of rigidity of polymer matrices and reduced nonradiative decay. We note that such an impact of rigidity of polymer matrices on the optical properties resembles some features of the structure−property relationship as revealed in green 1uorescent proteins,

https://doi.org/10.1021/acs.macromol.2c01199
Macromolecules 2022, 55, 8619−8628

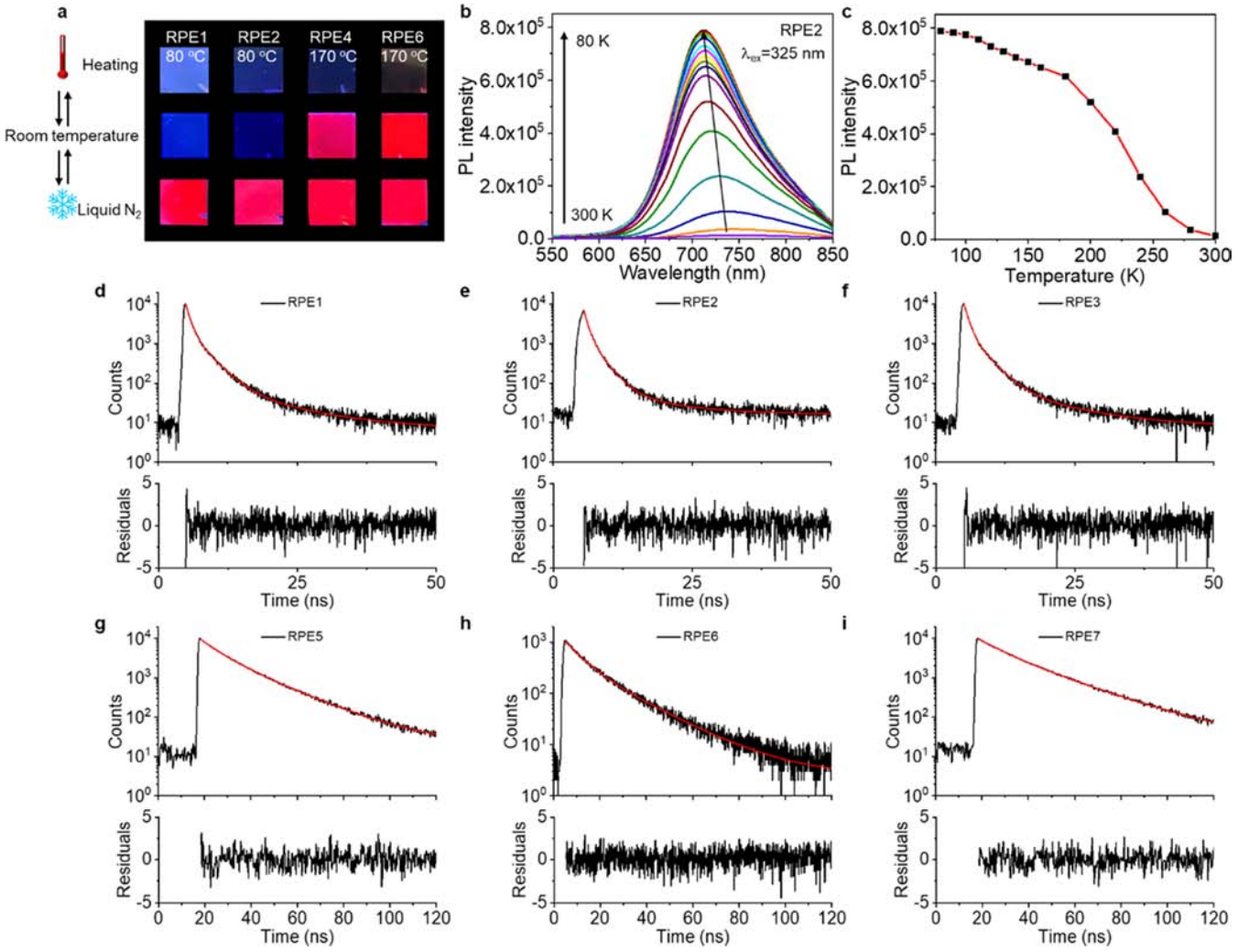

Figure 2. (a) Digital photographs of four RPE thin films on quartz slides under UV light (365 nm). (b) Temperature-dependent steady-state PL emission (λ_{ex} = 325 nm) spectra of the RPE2 film. (c) Evolution of the maximal PL intensity of the RPE2 film as a function of temperature. (d−i) Time-resolved PL decay profiles of RPE1−3, 5−7 in films at RT and their corresponding fit. The weighted residuals are shown as an indicator of the quality of the triple-exponential fitting.

in which the small Stokes shift, the high quantum yield of fluorescence, and the inability of O_2 to quench the excited states were proposed to be related with the rigid encapsulation of a single fluorophore inside a folded protein cylinder.[31]

We also studied the effect of MW of polyesters on the optical properties of radicals tethered by PCL (RPE2−3) or PLLA (RPE5−7). The optical absorption and steady-state PL emission spectra of RPE2−3 (Figure S21) show essentially the same Stokes shift for these two polymers as diluted solutions in toluene. Nevertheless, in solid films of these two polymers at 78 K, one can see an obviously smaller Stokes shift for RPE3 than that of RPE2. Given the fact that polymers with a larger MW (in the low to the moderate range) tend to have a higher T_g, the smaller Stokes shift is consistent with the restricted mobility of the radical core in the polymer matrices in solid states, which is also observed in Figure 1. Nevertheless, a larger Stokes shift was observed in the RPE3 film at RT, compared to that of the RPE2 film at the same temperature. Such apparently contradicting results imply that other factors such as crystallinity and transparency of the films may also affect the Stokes shift. Regarding RPE5−7, again no difference in the Stokes shift can be observed in a diluted solution in toluene (Figure S22). In solid films, all of RPE5−7 polymers show strong red PL under UV (365 nm) light irradiation at RT (Figure S23a). Nevertheless, while the RPE5 film appeared transparent, both RPE6 and RPE7 appeared opaque. As a result, the relatively strong light scattering effect in RPE6−7 would complicate a reliable analysis of the Stokes shift from the optical spectra (Figure S23b−d).

To understand the role of the fluorophore in the thermoresponsive behavior of the PL in polymeric matrices, we carried out a control experiment by examining the temperature dependence of the PL intensity of a PCL−DPP−PCL polymer (M_n = 28.9 kg/mol, PDI = 1.26), composed of a rigid fluorophore of thiophene-flanked diketopyrrolopyrrole (DPP) tethered from both ends.[32,33] Under 365 nm UV light irradiation, the thin films of PCL−DPP−PCL drop-cast on glass substrates maintain the intense yellow fluorescence at RT, or after being cooled down with liquid nitrogen, or being heated to 80 °C (Figure S24). Such low temperature-sensitivity of PCL−DPP−PCL, in contrast to the thermoresponsive PL of the RPE polymers as described above, suggests that the molecular structure of the fluorophore also plays a role in the thermal sensitivity of the polymer-tethered fluorophores.

https://doi.org/10.1021/acs.macromol.2c01199
Macromolecules 2022, 55, 8619−8628

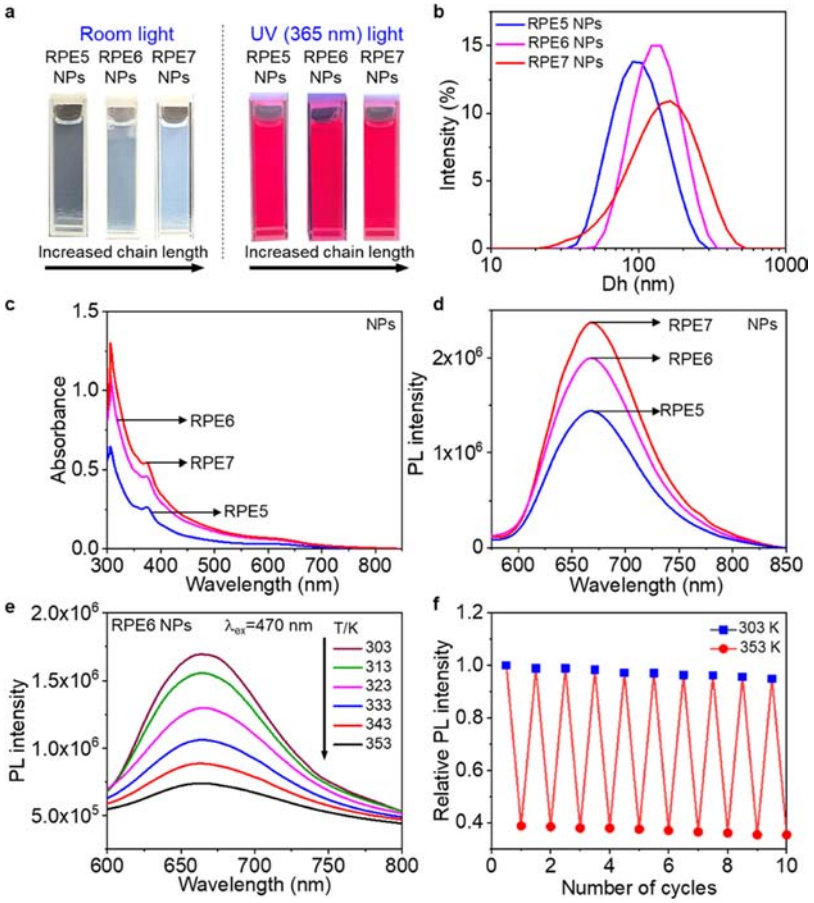

Figure 3. Characterization of radical-centered polyester nanoparticles (NPs) (a) digital photographs of RPE5, RPE6, and RPE7 NPs (1.25 mg mL RPE) in aqueous media under ambient and UV (365 nm) light. (b) Dynamic light scattering (DLS) histograms of the NPs in aqueous solution. (c) UV−vis absorption of NPs (1.25 mg mL RPE). Steady-state PL emission (λ_{ex} = 470 nm) spectra of RPE5−6 NPs at RT (d) and RPE6 NPs (1.25 mg mL) at different temperatures (e). (f) Evolution of the maximal PL intensity of RPE6 NPs during 10 heating−cooling cycles.

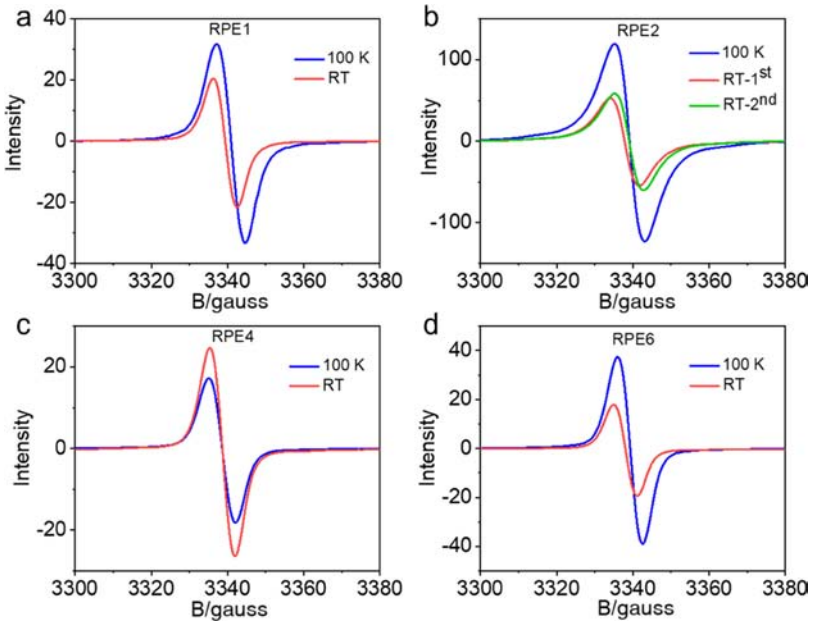

Figure 4. ESR spectra of four powder-state RPEs at room temperature (298 K) and 100 K, respectively.

To facilitate potential biorelated applications, we demonstrate the possibility of dispersing these radical-centered polyesters as colloidal nanoparticles (NPs) in water via a nanoprecipitation approach using an amphiphilic triblock copolymer Pluronic F127 as the stabilizer. Full details are given in the Supporting Information. The average hydrodynamic diameters of NPs

https://doi.org/10.1021/acs.macromol.2c01199
Macromolecules 2022, 55, 8619−8628

revealed by dynamic light scattering (DLS) were 9 (RPE5), 114 (RPE6), and 13 nm (RPE7) (Figure 3b). The polydispersity indices (PDI) of the three NPs were measured to be around .2, indicating good uniformity. The dispersions of both RPE6 and RPE7 NPs with increased chain lengths changed from transparency to milky white under ambient light (Figure 3a), which can be re1ected from the light scattering ef ect in the absorption spectra (Figures 3c and S25). All three NPs showed bright red emissions under UV light (365 nm) (Figure 3a). As the chain length increases, the emission intensity of the radical 1uorophore increases too (Figure 3d). No obvious emission shift of NPs was observed as the chain length was altered. Upon increase of the temperature, there was a decrease in the maximal intensity of the PL emission of the NPs (Figure 3e), while no signif cant change was observed in the maximal emission wavelengths (Figure S26). The 1uctuation of the PL intensity as observed in repeated heating−cooling cycles indicates good thermal stability of the NPs (Figure 3f).

Electron Spin Resonance of Radical-Centered Polyesters. Steady-state ESR spectra of representative RPE1, RPE2, RPE4, and RPE6 (Figure 4) were recorded in the powdered state at 298 and 1 K and compared with that of the TTM radical (Figure S28). Table 2 shows the g values and line widths

Table 2. SR Characteristics o RP Polymers

	298 K		1 K	
sample	g	ΔH_{pp}	g	ΔH_{pp}
RPE1	2.28	6.9	2.28	7.4
RPE2-1st	2.29	7.6	2.28	7.9
RPE2-2nd	2.28	9.3		
RPE3-1st	2.3	5.4	2.27	6.3
RPE3-2nd	2.28	5.3		
RPE4	2.29	6.6	2.28	7.
RPE6	2.29	6.2	2.28	6.6

(peak to peak line width, ΔH_{pp}) of these four RPEs. The measured spin concentrations of RPE polymers are in the range of $1^{18}-1^{21}$ spinsFg, which is signif cantly lower than that of the TTM radical (Table S2). These results are consistent with the dilution ef ect of polyesters on the radicals.

All recorded ESR spectra of RPEs show a single line with similar g values of 2.28 ± .2 (Table 2). In contrast to the asymmetric and broad line of the TTM radical in solid states (Figure S28), symmetric and relatively narrow lines were observed in RPE solids at both RT and 1 K (Figures 4 and S27). The absence of line splittings due to hyperf ne coupling in the ESR spectra of RPEs implies the possible spin−spin interactions in the solid states of these polymers. Other factors, such as the restricted motion of electron spins and the anisotropic nature of the polymeric matrices, may also contribute to the line broadening of the ESR spectra as observed here. Moreover, a broadening of the lines can be observed on decreasing the temperature and the polymer rigidity for all recorded RPEs (Figure 4 and Table 2). The temperature dependence can be attributed to the slower rotation of the electron spin and longer rotational correlation times of the radical-centered polyester at low temperatures.[23,34]

Finally, we compared the ESR properties of RPE2 (Figure 4b and Table 2) and RPE3 (Figure S27 and Table 2) with dif erent chain lengths of the PCL. The fact that RPE3 has a smaller ΔH_{pp} than RPE2 implies that RPE3 with a longer average chain length has a reduced rotation rate and an elongated rotational correlation time of the electron spins than those of RPE2. In addition, some hysteresis of the EPR signal was observed after being cooled down to 1 K and warmed back to RT (Figures 4b and S27). A further study of the structure−property relationship on individual spins dispersed in polymeric matrices is needed in the future using advanced techniques of pulsed ESR.

Tuning Photoluminescence by Plasticizers. To establish the relationship between the PL intensity of the radical-centered polyester with the T_g of the polymeric matrices, we selected both diethyl phthalate (DEP) as a commercially available industrial plasticizer (T_g K −85 °C)[35] and a synthetic plasticizer, a branched PCL (T_g K −62 °C)[36] (structure is shown in Figure S29), to lower the T_g of RPE6. The T_g of RPE6 is expected to be decreased, according to the Fox equation,[37] upon the increase of the weight ratios of the plasticizer.

The digital photographs of RPE6 f lms on glass substrates were recorded under room light and UV (365 nm) light before and after the addition of DEP (Figure 5a) and the branched PCL, respectively, (Figure 5b) with dif erent ratios and at dif erent temperatures. The f lm without the additional plasticizer remained highly luminescent until being heated up to 1 °C, where an obvious decrease in the luminescence intensity can be discerned. With the increase of the weight percentage of DEP from 17 to 46(, the luminescence intensity of the f lms at the same temperature appeared weaker gradually. Compared to DEP, the addition of the branched PCL had a much weaker impact on the luminescence of RPE6 f lms. Specif cally, the RPE6 f lm in the presence of 5 wt (of branched PCL remained vividly luminescent under UV light (365 nm) irradiation, in contrast to the obviously decreased luminescence in the presence of DEP with a similar percentage. Remarkably, the RPE6 f lm still showed visible pink luminescence when the percentage of the branched PCL was increased up to 97−98 wt (, although the average luminescence intensity appeared obviously weaker than that of the pristine RPE6 f lm at the same temperature. Signif cant luminescence quenching was observed in RPE6 f lms after addition of 99 wt (of the branched PCL (Figure 5b). These results further indicate the impact of the rigidity of the polymeric matrices, which is tunable by addition of plasticizers, on the photoluminescence of the TTM radicals in f lms.

Photostability of Radical-Centered Polymers. We further studied the photostability of RPE polymers, using RPE6 as a representative and a physically blended mixture of PLLA and the radical initiator (TTM-CZ-OH) as the control. All photostability investigations were performed in air. Recording the photos of f lms after dif erent exposure times to white LED light revealed rapid photobleaching of TTM-CZ-OH physically mixed in PLLA (Figure S3). The rates of photobleaching were obviously slower in RPE6 f lms than in the physically blended control sample. It has to be noted that in the control sample, severe phase separation appeared after 3 min of exposure to white LED light. In contrast to the vulnerability of the physical blend of TTM-CZ-OH and PLLA against photobleaching and phase separation, under similar conditions of light irradiation, both photobleaching and phase separation were signif cantly suppressed in RPE6 f lms where the radical is covalently linked at the center of each PLLA chain (Figure S3). The excellent photostability of RPE6 f lms under light irradiation implies su) cient protection of the radical center against 1uorescence quenchers such as O_2 and H_2O in air. These results demonstrate clear advantages of our polymer design by covalently tethering single radicals in the middle of polymer

https://doi.org/10.1021/acs.macromol.2c01199
Macromolecules 2022, 55, 8619−8628

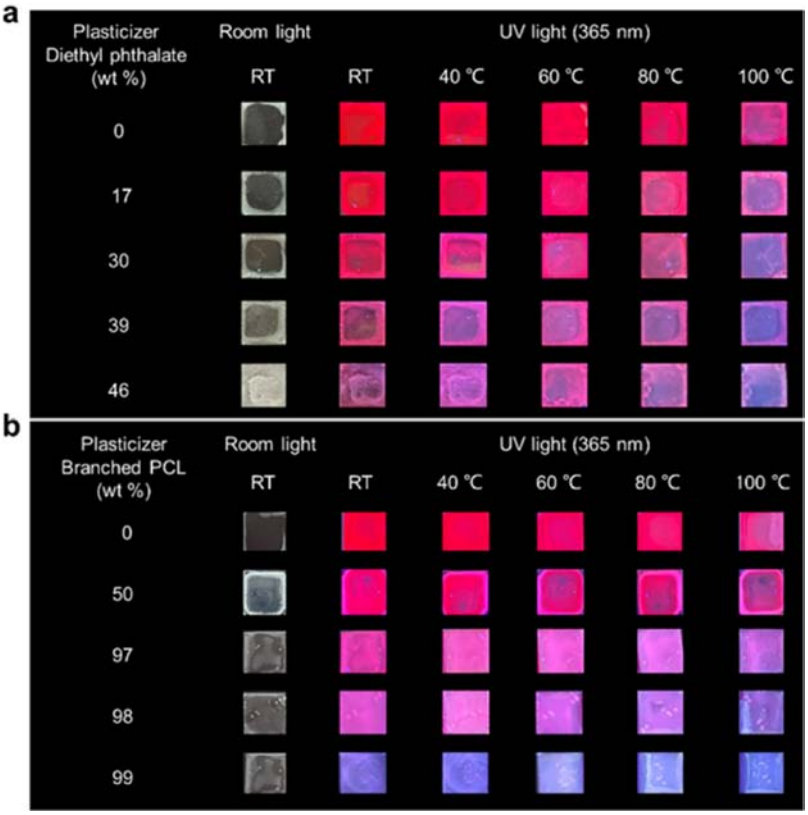

Figure 5. Digital photographs of RPE6 films under room light and UV (365 nm) light as a function of temperature before and after addition of plasticizers (a) diethyl phthalate and (b) branched PCL.

chains, which may benef t a broad range of applications such as light-emitting devices and quantum technologies involving the manipulation of single radical spins.

CONCLUSIONS

We have presented an ef ective synthetic strategy of suppressing inter-radical aggregation and controlling electron spin dynamics by molecular design and synthesis of a series of carbazole-triphenylmethyl-based radicals tethered with polyesters. Our experimental results demonstrate that the rigidity of the polymeric matrices has a signif cant impact on the photoluminescence and electron spin resonance of the radicals in solid states. Polylactides with a relatively high T_g lead to strong red-to-NIR photoluminescence with a lifetime of 14−18 ns at room temperature, and an electron spin correlation time longer than that of the same type of radicals tethered with polylactones with a lower T_g. The radicals tethered with polylactones show weak photoluminescence with a short lifetime of 2.−2.4 ns at room temperature. After being chilled with liquid nitrogen, these polylactones regain the photoluminescence intensity and lifetime comparable to those of polylactide-tethered radicals. The impact of the rigidity of polymer matrices on the photoluminescence of the tethered radicals was further corroborated by the addition of plasticizers to lower the T_g of polylactide matrices. The tunable photoluminescence and electron spin dynamics, as well as the robust photostability of these polymer-tethered single radicals with well-def ned molecular structures, represent important attributes for applications in light-emitting devices, quantum information processing, and beyond.

ASSOCIATED CONTENT

Supporting Information

The Supporting Information is available free of charge at https://pubs.acs.org/doi/10.1021/acs.macromol.2c01199.

Experimental procedures; chemical synthesis and characterization of compounds; and supporting f gures (PDF)

AUTHOR INFORMATION

Corresponding Author

Mingfeng Wang − *School of Science and Engineering, The Chinese University of Hong Kong, Shenzhen 518172, China*; orcid.org/0000-0002-6445-6854; Email: wangmingfeng@cuhk.edu.cn

Authors

Liman Hou − *School of Science and Engineering, The Chinese University of Hong Kong, Shenzhen 518172, China*

Hongxue Xu − *School of Science and Engineering, The Chinese University of Hong Kong, Shenzhen 518172, China*

Xuanyu Zhang − *Department of Electrical and Electronic Engineering, Southern University of Science and Technology, Shenzhen 518055, China*

Yipeng Zhang − *School of Science and Engineering, The Chinese University of Hong Kong, Shenzhen 518172, China*

Rui Chen − *Department of Electrical and Electronic Engineering, Southern University of Science and Technology, Shenzhen 518055, China*; orcid.org/0000-0002-0445-7847

Zhaoyu Zhang − *School of Science and Engineering, The Chinese University of Hong Kong, Shenzhen 518172, China*; orcid.org/0000-0003-0335-0535

https://doi.org/10.1021/acs.macromol.2c01199
Macromolecules 2022, 55, 8619−8628

Complete contact information is available at3 https3FFpubs.acs.orgF1X.1X21Facs.macromol.2cX1199

Notes

The authors declare no competing f nancial interest.
The draft of an early version of the manuscript was deposited at ChemRxiv (DOI31X.26434Fchemrxiv-2X22-b8x9).

BX C4X O5 LEX 6 MEX TS

M.W. acknowledges the f nancial support from the University Development Fund-Research Start-Up Fund (UDFX1XX18X6) from the Chinese University of Hong Kong, Shenzhen. The authors thank the Advanced Materials Laboratory and the School of Science and Engineering for access to instrumental platforms such as spectrometers and gel-permeation chromatography. They also thank the School of Life and Health Sciences for access to the 1uorometer. H.X. thanks f nancial support of her Ph.D. Scholarship from the Chinese University of Hong Kong, Shenzhen.

BRE3ERE X CES

(1) Hicks, R. G. *Stable X adicalsXX undamentals and Applied Aspects of X dd, Electron Compounds*; John Wiley P Sons Ltd.3 Chichester, U.K., 2X1X; pp 1−588.
(2) Ratera, I.; Veciana, J. Playing with organic radicals as building blocks for functional molecular materials. *Chem. Soc. X ev.* **2012**, *. 1*, 3X3−349.
(3) Yuan, D.; Liu, W.; Zhu, X. Design and Applications of Single-Component Radical Conductors. *Chem* **2021**, *7*, 333−357.
(4) Ji, L.; Shi, J.; Wei, J.; Yu, T.; Huang, W. Air-Stable Organic Radicals3 New-Generation Materials for Flexible ElectronicsQ *Adv. Mater.* **2020**, *32*, 19X8X15−19X8X29.
(5) Hu, X.; Wang, W.; Wang, D.; Zheng, Y. The electronic applications of stable diradicaloids3 present and future. *J. Mater. Chem. C* **2018**, *6*, 11232−11242.
(6) Yang, K.; Zhang, X.; Harbuzaru, A.; Wang, L.; Wang, Y.; Koh, C.; Guo, H.; Shi, Y.; Chen, J.; Sun, H.; Feng, K.; Ruiz Delgado, M. C.; Woo, H. Y.; Ortiz, R. P.; Guo, X. Stable Organic Diradicals Based on Fused L uinoidal Oligothiophene Imides with High Electrical Conductivity. *J. Am. Chem. Soc.* **2020**, *1. 2*, 4329−434X.
(7) Gopalakrishna, T. Y.; Zeng, W.; Lu, X.; Wu, J. From open-shell singlet diradicaloids to polyradicaloids. *Chem. Commun.* **2018**, *5. *, 2186−2199.
(8) Chen, Z. X.; Li, Y.; Huang, F. Persistent and Stable Organic Radicals3Design, Synthesis, and Applications. *Chem* **2021**, *7*, 288−332.
(9) Gamero, V.; Velasco, D.; Latorre, S.; LRpez-Calahorra, F.; Brillas, E.; JuliS, L. T4-(N-Carbazolyl)-2,6-dichlorophenyl Ubis(2,4,6-trichlorophenyl)methyl radical an efficient red light-emitting paramagnetic molecule. *Tetrahedron 2ett.* **2006**, *. 7*, 23X5−23X9.
(1X) Hattori, Y.; Kusamoto, T.; Nishihara, H. Luminescence, stability, and proton response of an open-shell (3,5-dichloro-4-pyridyl)bis(2,4,6-trichlorophenyl)methyl radical. *Ang2. Chem., Int.* Ed. **2014**, *53*, 11845−11848.
(11) Peng, L.; Obolda, A.; Zhang, M.; Li, F. Organic light-emitting diodes using a neutral πradical as emitter3the emission from a doublet. *Ang2. Chem., Int.* Ed. **2015**, *5. *, 7X91−7X95.
(12) Ai, X.; Evans, E. W.; Dong, S.; Gillett, A. J.; Guo, H.; Chen, Y.; Hele, T. J. H.; Friend, R. H.; Li, F. Efficient radical-based light-emitting diodes with doublet emission. *Nature* **2018**, *563*, 536−54X.
(13) Abdurahman, A.; Hele, T. J. H.; Gu, L.; Zhang, J.; Peng, L.; Zhang, M.; Friend, R. H.; Li, F.; Evans, E. W. Understanding the luminescent nature of organic radicals for efficient doublet emitters and pure-red light-emitting diodes. *Nat. Mater.* **2020**, *16*, 1224−1229.
(14) Cui, Z.; Abdurahman, A.; Ai, X.; Li, F. Stable Luminescent Radicals and Radical-Based LEDs with Doublet Emission. *CCS Chem.* **2020**, *2*, 1129−1145.
(15) Liu, C. H.; Hamzehpoor, E.; Sakai-Otsuka, Y.; Jadhav, T.; Perepichka, D. F. A Pure-Red Doublet Emission with 9X(L uantum Yield3 Stable, Colorless, Iodinated Triphenylmethane Solid. *Ang2. Chem., Int.* Ed. **2020**, *56*, 23X3X−23X34.
(16) Simão, C.; Mas-Torrent, M.; Crivillers, N.; Lloveras, V.; ArtVs, J. M.; Gorostiza, P.; Veciana, J.; Rovira, C. A robust molecular platform for non-volatile memory devices with optical and magnetic responses. *Nat. Chem.* **2011**, *3*, 359−364.
(17) Mothika, V. S.; Baumgarten, M.; Scherf, U. Neutral, π-Radical-Conjugated Microporous Polymer Films of Nanoscale Thickness for Potential Use in Magnetoelectronics and Sensor Devices. *ACS Appl. Nano Mater.* **2019**, *2*, 4832−4841.
(18) Kato, K.; Osuka, A. Platforms for Stable Carbon-Centered Radicals. *Ang2. Chem., Int.* Ed. **2019**, *58*, 8978−8986.
(19) Kato, K.; Kimura, S.; Kusamoto, T.; Nishihara, H.; Teki, Y. Luminescent Radical-Excimer3Excited-State Dynamics of Luminescent Radicals in Doped Host Crystals. *Ang2. Chem., Int.* Ed. **2019**, *58*, 26X6−2611.
(2X) Dai, Y. Z.; Dong, B. W.; Kao, Y.; Wang, Z. Y.; Un, H. I.; Liu, Z.; Lin, Z. J.; Li, L.; Xie, F. B.; Lu, Y.; Xu, M. X.; Lei, T.; Sun, Y. J.; Wang, J. Y.; Gao, S.; Jiang, S. D.; Pei, J. Chemical Modification toward Long Spin Lifetimes in Organic Conjugated Radicals. *ChemPhysChem* **2018**, *16*, 2972−2977.
(21) Kimura, S.; Kimura, S.; Nishihara, H.; Kusamoto, T. Excimer emission and magnetoluminescence of radical-based zinc(II) complexes doped in host crystals. *Chem. Commun.* **2020**, *56*, 11195−11198.
(22) Kimura, S.; Uejima, M.; Ota, W.; Sato, T.; Kusaka, S.; Matsuda, R.; Nishihara, H.; Kusamoto, T. An Open-shell, Luminescent, Two-Dimensional Coordination Polymer with a Honeycomb Lattice and Triangular Organic Radical. *J. Am. Chem. Soc.* **2021**, *1. 3*, 4329−4338.
(23) Jellen, M. J.; Ayodele, M. J.; Cantu, A.; Forbes, M. D. E.; Garcia-Garibay, M. A. 2D Arrays of Organic L ubit Candidates Embedded into a Pillared-Paddlewheel Metal-Organic Framework. *J. Am. Chem. Soc.* **2020**, *1. 2*, 18513−18521.
(24) Le Devedec, F.; Boucher, H.; Dubins, D.; Allen, C. Factors Controlling Drug Release in Cross-linked Poly(valerolactone) Based Matrices. *Mol. Pharmaceutics* **2018**, *15*, 1565−1577.
(25) Chien, Y. C.; Chuang, W. T.; Jeng, U. S.; Hsu, S. H. Preparation, Characterization, and Mechanism for Biodegradable and Biocompatible Polyurethane Shape Memory Elastomers. *ACS Appl. Mater. Interfaces* **2012**, *6*, 5419−5429.
(26) Zhang, J.; Tashiro, K.; Tsuji, H.; Domb, A. J. Investigation of Phase Transitional Behavior of Poly(L-lactide)FPoly(D-lactide) Blend Used to Prepare the Highly-Oriented Stereocomplex. *Macromolecules* **2002**, *. X, 1X49−1X54.
(27) BSez, J. E.; Marcos-FernSndez, A. A Comparison of Three Different Biodegradable Aliphatic Oligoesters (PGA, PLLA, and PCL) with Similar Linear Alkyl End Groups by DSC and SAXS. *Int. J. Polym. Anal. Charact.* **2015**, *2X*, 637−644.
(28) Suzuki, Y.; Watanabe, T.; Kosugi, H.; Ueda, K.; Kikuchi, M.; Narumi, A.; Kawaguchi, S. Chain Conformation of Poly(d-lactide) in Tetrahydrofuran by Static Light Scattering, Small-Angle X-ray Scattering, and Intrinsic Viscosity. *Macromolecules* **2020**, *53*, 16X4−1612.
(29) Saito, Y.; Izuta, D.; Kaneko, N.; et al. Molecular Characterization of Poly (L-lactic acid) Isolated Chain. *Kobunshi Xonbunshu* **2012**, *66*, 416−423.
(3X) Suzuki, Y.; Watanabe, T.; Kosugi, H.; Ueda, K.; Kikuchi, M.; Narumi, A.; Kawaguchi, S. Dilute solution properties of poly(d,l-lactide) by static light scattering, SAXS, and intrinsic viscosity. *Polym. J.* **2020**, *52*, 387−396.
(31) OrmW M.; Cubitt, A. B.; Kallio, K.; Gross, L. A.; Tsien, R. Y.; Remington, S. J. Crystal Structure of the *Ae8uorea victoria* Green Fluorescent Protein. *Science* **1996**, *273*, 1392−1395.
(32) Wang, K.; Luo, Y.; Huang, S.; Yang, H.; Liu, B.; Wang, M. Highly Fluorescent Polycaprolactones Decorated with Di(thiophene-2-yl)-diketopyrrolopyrrole3 A Covalent Strategy of Tuning Fluorescence Properties in Solid States. *J. Polym. Sci., Part A Polym. Chem.* **2015**, *53*, 1X32−1X42.

(33) Huang, S.; Liu, S.; Wang, K.; Yang, C.; Luo, Y.; Zhang, Y.; Cao, B.; Kang, Y.; Wang, M. Highly fluorescent and bioresorbable polymeric nanoparticles with enhanced photostability for cell imaging. *Nanoscale* **2015**, *7*, 889−895.
(34) Xia, Y.; Li, Y.; Burts, A. O.; Ottaviani, M. F.; Tirrell, D. A.; Johnson, J. A.; Turro, N. J.; Grubbs, R. H. EPR Study of Spin Labeled Brush Polymers in Organic Solvents. *J. Am. Chem. Soc.* **2011**, *133*, 19953−19959.
(35) Rowe, R. C.; Kotaras, A. D.; White, E. F. T. An evaluation of the plasticizing efficiency of the dialkyl phthalates in ethyl cellulose films using the torsional braid pendulum. *Int. J. Pharm.* **1984**, *22*, 57−62.
(36) Choi, W.; Chung, J. W.; Kwak, S. Y. Unentangled star-shape poly(ε-caprolactone)s as phthalate-free PVC plasticizers designed for non-toxicity and improved migration resistance. *ACS Appl. Mater. Interfaces* **2014**, *6*, 11118−11128.
(37) Fox, T. G. Influence of diluent and copolymer composition on the glass temperature of a polymer system. *Bull. Am. Phys. Soc.* **1956**, *1*, 123−128.

https://doi.org/10.1021/acs.macromol.2c01199
Macromolecules 2022, 55, 8619−8628